

Electrochemical Detection of Single Nucleotide Polymorphism in Short DNA Sequences Related To Cattle *Fatty Acid Binding Protein 4* Gene

Venu Reddy¹, Torati Sri Ramulu¹, Brajalal Sinha¹, Jaein Lim¹, Md. Rashedul Hoque², Jun-Heon Lee², ChoelGi Kim^{1,*}

¹ Department of Materials Science and Engineering, Chungnam National University, Daejeon 305-764, South Korea.

² Department of Animal Science and Biotechnology, Chungnam National University, Daejeon 305-764, South Korea

*E-mail: cgkim@cnu.ac.kr

Received: 13 September 2012 / Accepted: 12 October 2012 / Published: 1 November 2012

Electrochemical nucleic acid biosensor for detection of single nucleotide polymorphism (SNP) in *Fatty acid binding protein 4 (FABP4)* has been developed by immobilization of single stranded thiolated probe DNA (ss-DNA-SH) onto gold surfaces (ss-DNA-SH/Au) and its hybridization with wild and mutant complementary sequences related to Korean cattle *FABP4* gene in the presence methylene blue. The immobilization of ss-DNA-SH onto gold surfaces was characterized by atomic force microscopy (AFM), Fourier transforms infrared microscopy (FT-IR), cyclic voltammetric (CV) and impedance techniques. The SNP in Korean cattle *FABP4* gene was detected by measuring the methylene blue accumulation on ss-DNA-SH/Au electrode hybridized with wild (wild-ds-DNA-SH/Au) and mutant (mutant-ds-DNA-SH/Au) complementary sequences using CV technique. The sensitivities of wild-ds-DNA-SH/Au and mutant-ds-DNA-SH/Au electrodes are $0.0164 \mu\text{A}/\text{ng} \mu\text{L}^{-1}$ with 0.998 regression coefficient (R) and $0.0122 \mu\text{A}/\text{ng} \mu\text{L}^{-1}$ with 0.993 R, respectively. The ssDNA-SH/Au electrode can detect the wild and mutant type complementary targets related to *FABP4* gene in the range of 5-10 ng μL^{-1} .

Keywords: *FABP4* gene, Electrochemical DNA biosensor, Single nucleotide polymorphism, Korean cattle

1. INTRODUCTION

Fatty acid binding protein 4 (FABP4) is a candidate gene affecting fatness traits of mammals and expresses the *FABP4*. The *FABP4* is a highly conserved cytoplasmic protein that can bind long-

chain fatty acids and other hydrophobic ligands [1]. Their major functions include intracellular free fatty acid transport and metabolism. Fatty acid trafficking during lipolysis is mediated by *FABP4*, and the binding with hormone-sensitive lipase is the primary step in an organized lipid-transfer process [2]. The single nucleotide polymorphisms (SNPs) in *FABP4* gene effects on the carcass weight of the cattle due to variation in the intramuscular fat content [3]. In the beef industry, the intramuscular fat content in the meat cattle is an important trait to improve the nutritional values of the meat cattle. Thus, the detection of in the *FABP4* gene is significant to improve the nutritional values of the meat cattle.

Since, several techniques have been developed for the detection of SNPs in DNA. Traditional procedures involved the implementation of mass spectroscopy or gel electrophoresis for the discrimination of DNA fragments produced by enzyme cleavage [4-5]. Jisan et al. described a novel colorimetric method for SNP detection using high fidelity DNA ligase. This approach has a capability to detect the single base discrimination without need of precise temperature control [6]. Li et al. reported a nanoparticle-enhanced surface plasmon resonance imaging measurements of surface enzymatic ligation reaction for the detection of SNP in DNA [7]. For detection of SNPs in *FABP4*, many researchers have been using genetic analyzers [2,7-8]. For instance, Lee et al. identified 16 SNPs in *FABP4* gene. Among these 16 SNPs, the g.3473A>T SNP showed a significant increasing effect on the carcass weight of the Korean cattle [7]. Nevertheless, these techniques are suffering from some limitations such as time consuming and need the higher mass volume of sample and high cost equipments [6]. Therefore, there is great demand to develop the methods for SNPs detection that are simple, inexpensive and readily amenable to high throughput automatic analysis.

The electrochemical detection of SNPs has been recently received more attention due to its high sensitivity, economical and suitability for compact and portable device [9]. The use of redox molecule, methylene blue (MB) is interesting in the electrochemical detection of SNPs due to their high affinity towards nucleic acids. In the literature, three different mechanisms of MB-DNA interaction have been reported: (i) electrostatic interaction with negatively charged DNA backbone, (ii) intercalation between the two DNA strands and (iii) preferential binding to free guanine bases within the single-stranded DNA (ssDNA) [10-14]. So far, a very few reports can be found in the literature for electrochemical detection of SNP using methylene blue as redox material. Oliver et al. reported the methylene based detecting method for SNP by using DNA targets of equal length to the probe DNA [15]. Shana et al. describe the charge transfer through DNA films was exploited for the electrochemical detection of SNP, which was detected by the reduction in the electron transfer that they generated in a double stranded DNA film immobilized onto a gold electrode and having MB intercalated [16]. However, to our knowledge, there are no reports on electrochemical detection of SNP in cattle genes using methylene blue.

Here, we report the methylene blue based electrochemical detection of SNP in the cattle *FABP4* gene responsible for intramuscular fat content in the meat cattle using a synthetic complementary DNA sequence (24 bases) as the model targets. In this study, we described the results relating to immobilization of thiol labeled DNA probe (24 bases) onto the gold surfaces and the use of methylene blue for SNP detection in mutant and wild type complementary DNA sequences relating to cattle *FABP4* gene during the hybridization process.

2. EXPERIMENTAL

2.1. Materials

Methylene blue, Potassium ferricyanide $K_3[Fe(CN)_6]$, potassium ferrocyanide $K_4[Fe(CN)_6]$, and Tris-EDTA buffer (pH 8) was obtained from Sigma Aldrich, USA. Other chemicals were of analytical grade. The 24-mer oligonucleotides of the thiolated probe DNA (ssDNA-SH) and wild and mutant type of complementary targets DNA (ssDNA) were procured (as lyophilized) from GeneChem Inc, Korea. The base sequences are as follows:

- i) Thiolated probe DNA: 5'-TCT TAT CAT CCA TGA GTT TTC TCT-(CH₂)₃-SH-3'
- ii) Wild type complementary target DNA: 5'-AGA GAA AAC TCG TGG ATG ATA AGA-3'
- iii) Mutent type complementary target DNA: 5'-AGA GAA AAC TCA TGG ATG ATA AGA-3'

The stock solutions of DNA were prepared in Tris-EDTA buffer (pH 8). Other reagents were prepared in de-ionized water (Milli-Q). A 0.05 M phosphate buffer saline (PBS) solution was prepared using Na_2HPO_4 (0.2 M) and NaH_2PO_4 (0.2 M) with 0.15 M of NaCl.

2.2. Apparatus

The gold electrodes were fabricated using DC magnetron sputtering system. Electrochemical measurements were performed using an Autolab (EchoChemie, Netherlands) potentiostat/galvanostat. The electrochemical cell consisted of a three electrode system with a gold electrode as working electrode, an Ag/AgCl reference electrode and a platinum sheet counter electrode. The surface topographies of bare Au and ssDNA-SH/Au were delineated using atomic force microscopy (AFM) (Asylum Research, USA) in tapping mode. Fourier transform infrared (FTIR) spectra were recorded using an attenuated total reflectance instrument (Bruker Optic GmbH, Germany) for the DNA immobilization on gold electrode.

2.3. Methods

2.3.1. Fabrication of gold electrodes

The gold electrodes were fabricated by sputtering of Ta(10 nm)/Au(180 nm) structure on the glass wafer (1 x 2 cm²) using a DC magnetron sputtering system with working pressure 3 mtorr.

2.3.2 Immobilization of Probe DNA (ssDNA-SH) on gold electrodes

Prior to immobilization, the electrode was cleaned with a piranha solution (70% H₂SO₄ and 30 % H₂O₂) for 10 min, dipping in 70% ethyl alcohol for 5 min, washed with water and dried at room temperature. Then, immobilized the thiolated probe DNA (ssDNA-SH) on the cleaned gold electrodes dispensing 10 μ L of 50 ng/ μ L probe DNA solution on the surface of gold electrodes and kept in the

humidification chamber for 12 h. After, the electrode was washed with Tris-EDTA buffer to remove any unbound probe DNA.

2.3.3 Hybridization of complementary wild and mutant targets

The complementary wild and mutant targets (ssDNA) relating to cattle *FABP4* gene was hybridized for 1 h at 37 °C with probe DNA immobilized on the gold electrode. After hybridization, the electrodes were washed with Tris-EDTA buffer to remove unhybridized complementary wild and mutant targets DNA. The electrode was stored at 4 °C, when it is not in use.

2.3.4. Electrochemical measurements

For immobilization studies, the cyclic voltammetry (CV) and electrochemical impedance (EI) measurements were performed in 5 mM $[\text{Fe}(\text{CN})_6]^{3-/4-}$ electrolyte solution, which was prepared in phosphate buffer saline (0.05 M PBS, pH 7.4). The impedance spectra of real and imaginary parts of impedance, $Z'(f)$ and $Z''(f)$, were obtained by EI measurements sweeping the frequency (f) of AC voltage with 10 mV amplitude in the range from 0.1 mHz to 10 kHz under the fixed DC voltage of 0.23 V. In SNP detection studies, the methylene blue accumulation on electrodes was measured by CV in 40 μM methylene blue solution, which was prepared in phosphate buffer saline (0.05 M PBS, pH 7.4). All the CV measurements were carried out at the scan rate of 20 mV/s. All the electrochemical studies were performed at room temperature.

3. RESULTS AND DISCUSSION

3.1. Immobilization studies

3.1.1. AFM studies

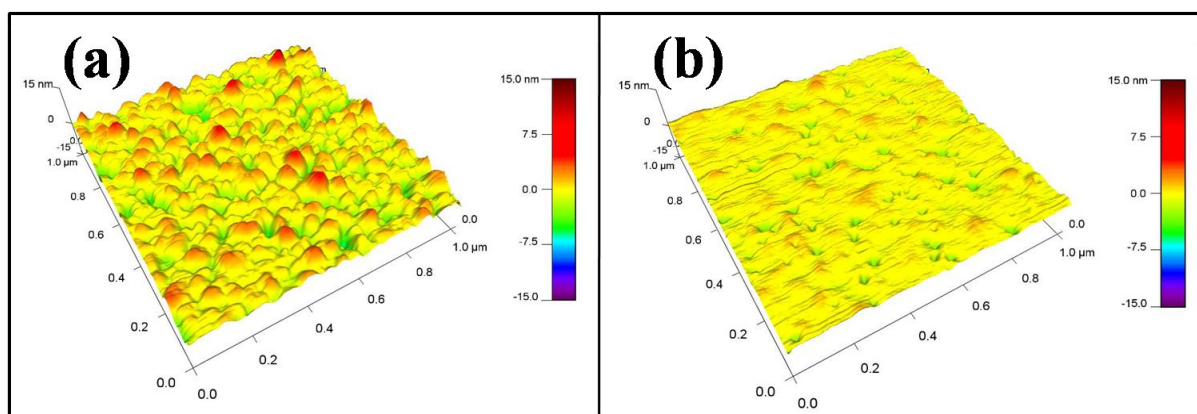


Figure 1.(a) AFM images of bare gold and (b) after immobilization of thiolated DNA (ss-DNA-SH-Au).

The AFM images of bare gold and Au/ssDNA-SH electrodes are shown in Fig. 1a and b, respectively. The bare gold AFM image shows the uniform distribution of granular nanoporous surface morphology with an average roughness of 1.510 nm (Fig. 1a). After, immobilization of thiolated probe DNA onto the gold surface, the granular nanoporous morphology on the gold surface changes to smooth nanoporous surface morphology with an average roughness of 0.732 nm (Fig. 1b). It indicates that the immobilization of thiolated probe DNA onto the gold surfaces.

3.1.2. FT-IR studies

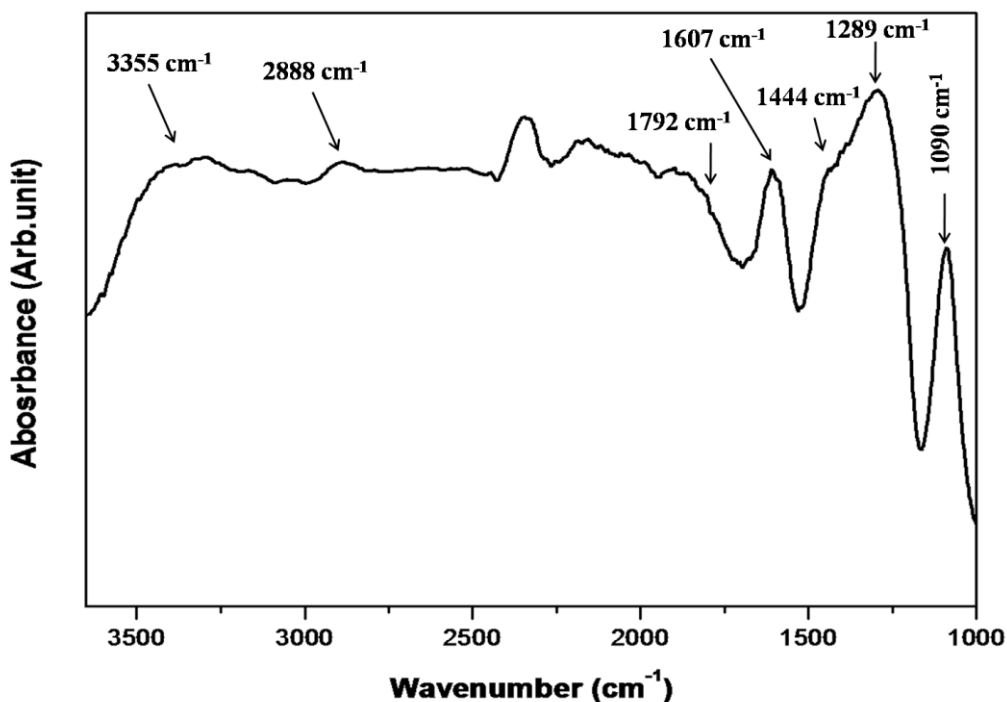


Figure 2. FT-IR spectra of ss-DNA-SH-Au electrode.

The FT-IR spectra of Au/ssDNA-SH electrode is shown in Fig. 2. The absorption peaks observed at 1090 and 1289 cm^{-1} correspond to asymmetric and symmetric vibrations of PO_4^- groups of the phosphodiester deoxyribose backbone in the ssDNA-SH. The absorption peaks at 1444, 1607, and 1792 cm^{-1} , which corresponds to cytosine, thymine and guanine bases respectively. In the present study, the absorption peak corresponding to adenine at 1525 cm^{-1} is not observed because it is merged in the thymine base peak. The absorption peak seen 2888 cm^{-1} is assigned to C-H bond in the ssDNA-SH. The peak at 3355 cm^{-1} is attributed to N-H stretching vibration of purine and pyrimidine rings in DNA bases [17-18]. These results indicate that ssDNA-SH probe is successfully immobilized on the gold electrode surfaces.

3.1.3. Cyclic voltammetric and electrochemical impedance studies

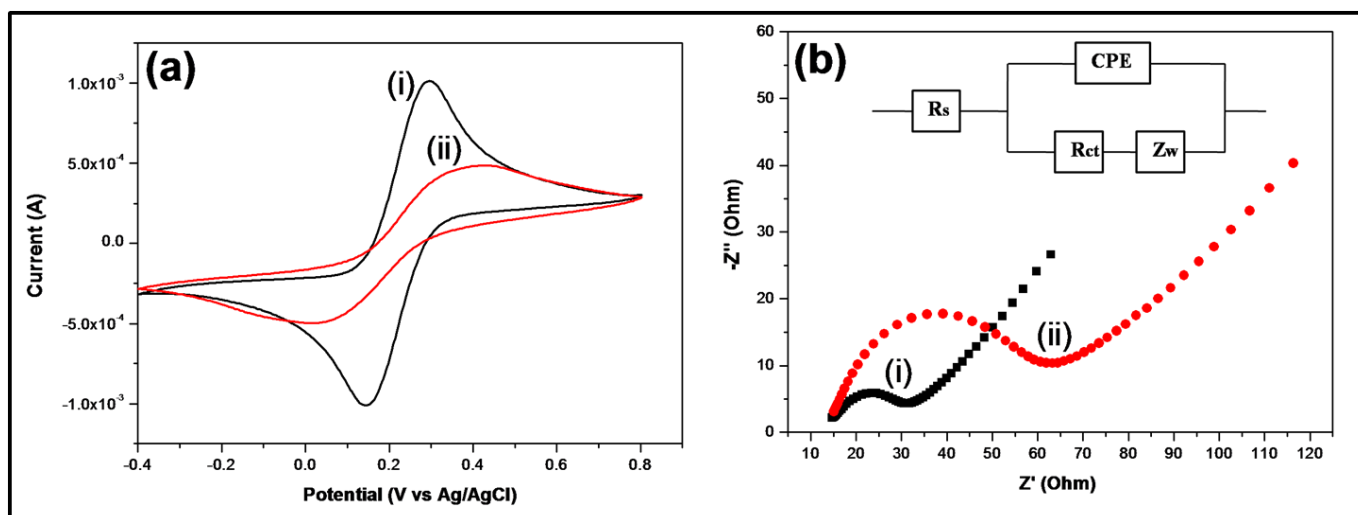


Figure 3. (a) Cyclic voltammograms and (b) Nyquist plots of (i) bare Au and (ii) after immobilization of thiolated DNA (ss-DNA-SH-Au) in PBS containing 5 mM $[\text{Fe}(\text{CN})_6]^{3-/4-}$. The inset in (b) represents an equivalent open circuit of EI measurements

The cyclic voltammograms of bare gold electrode (curve i) and ssDNA-SH/Au electrode (curve ii) are shown in Fig. 3a. The bare gold electrode produces a well defined anodic and cathodic peak potential at 0.296 to 0.143 V, respectively. The anodic peak current of bare gold is 0.001 A (curve i). After, immobilization of thiolated probe DNA onto the gold surface, the anodic peak current decreases to 0.384 A (curve ii), indicating that the probe DNA was successfully immobilized on the gold surfaces. Perhaps, the decrease of this anodic peak current is due to the repulsion between $[\text{Fe}(\text{CN})_6]^{3-/4-}$ species and the negatively charged phosphate back bone of the probe DNA onto the gold electrode (ssDNA-SH/Au).

The Nyquist plots from the EI measurements of bare gold (curve i) and ssDNA-SH/Au (curve ii) electrodes are shown in Fig. 3b. The equivalent open circuit for these EI measurements is shown in inset Fig. 3b. The R_{ct} values 16.41 (curve i) and 48.79 Ω (curve ii) are obtained for bare gold and ssDNA-SH/Au electrode, respectively. The ssDNA-SH/Au electrode R_{ct} value is high (large semicircle diameter) with respect to the bare gold electrode (small semicircle diameter). It reveals that slower electron-transfer kinetics is occurring on the ssDNA-SH/Au electrode in comparison to the bare gold electrode. This slower electron-transfer kinetics on the ssDNA-SH/Au electrode may be occurring due to the repulsion between the $[\text{Fe}(\text{CN})_6]^{3-/4-}$ and negatively charged DNA on the gold electrode (ssDNA-SH/Au) [19]. It confirms that the probe DNA was successfully immobilized onto the gold surfaces.

3.2. Single base-pair mismatch electrochemical detection studies

Fig. 4a displays CV measurements of ssDNA-SH/Au electrode (curve i), hybridized mutant type complementary target (mutant-dsDNA-SH/Au) (curve ii) and wild type complementary target (wild-dsDNA-SH/Au) (curve iii) related to *FABP4* gene to thiolated probe DNA onto the gold surface.

The ssDNA-SH/Au electrode anodic peak current value ($0.86 \mu\text{A}$) is lower compared to the mutant-dsDNA-SH/Au ($1.40 \mu\text{A}$) and wild-dsDNA-SH/Au ($1.61 \mu\text{A}$), indicating the methylene blue accumulation is more in dsDNA-SH/Au electrodes with respect to ssDNA-SH/Au electrode.

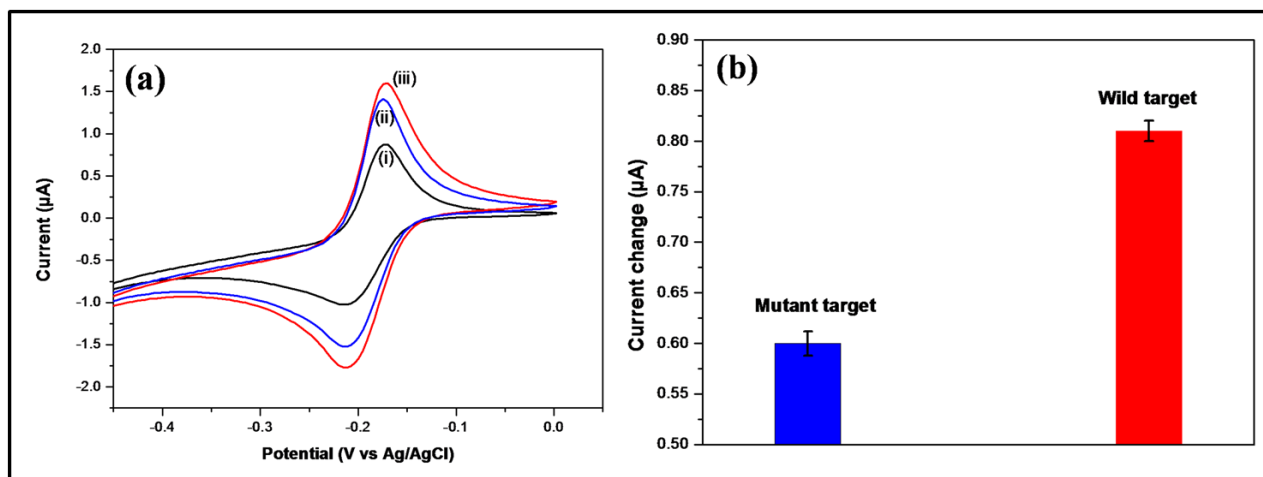


Figure 4. (a) Cyclic voltammograms of (i) ss-DNA-SH-Au, (ii) hybridization with mutant type DNA target (mutant-ds-DNA-SH-Au) and (iii) hybridization with wild type DNA target (wild-ds-DNA-SH-Au) in PBS containing $40 \mu\text{M}$ methylene blue. (b) Probe anodic peak current subtracted response to wild and mutant type complementary targets.

Generally, the methylene blue accumulation is more in the electrodes having ssDNA than that of electrodes having dsDNA, because the methylene blue has strong interaction with unpaired nitrogen bases present in the ssDNA (especially guanine bases) [20]. Here in our study, the methylene blue accumulation is more in the electrodes having dsDNA than that of the electrodes having ssDNA. This may be due to positively charged methylene blue is electrostatically interacted to negatively charged phosphate backbone of dsDNA and also the methylene blue is intercalated between the double helix as a result the methylene blue accumulation is higher in the electrodes having dsDNA with respect to the methylene blue accumulated due to unpaired nitrogen bases present in the electrodes having ssDNA [16].

On the other hand, the anodic peak current of the wild-dsDNA-SH/Au electrode is higher compared to that the mutant-dsDNA-SH/Au electrode. The ssDNA-SH/Au electrode anodic peak current subtracted response to the wild-dsDNA-SH/Au electrode and mutant-dsDNA-SH/Au electrode is shown in bar graph Fig. 4b. This variation in the anodic peak currents of the wild-dsDNA-SH/Au and mutant-dsDNA-SH/Au electrodes can be assigned to the methylene blue, which have a strong association with the guanine base at 12 position of wild type complementary target from 5' end and weak association with the adenine base at 12 position of mutant type complementary target from 5' end. This result provides the present method has the capability to recognize the SNP in *FABP4* gene and also generating a type of an electrochemical biosensor for the sequence detection in DNA.

The effect of wild and mutant type complementary target concentration on hybridization with probe DNA was also observed in Fig. 5. The wild (Fig. 5a) and mutant type (Fig. 5b) target

concentrations were increased from 10 to 50 ng/uL, the anodic peak currents of methylene blue were also increased. It reveals that the accumulation of methylene blue increases with an increase in the concentration of dsDNA. This may be due to that, when the concentration of dsDNA increases the methylene blue binds to the phosphate backbone of dsDNA and intercalation between the two strands of DNA, as a result the anodic peak current of methylene blue increases.

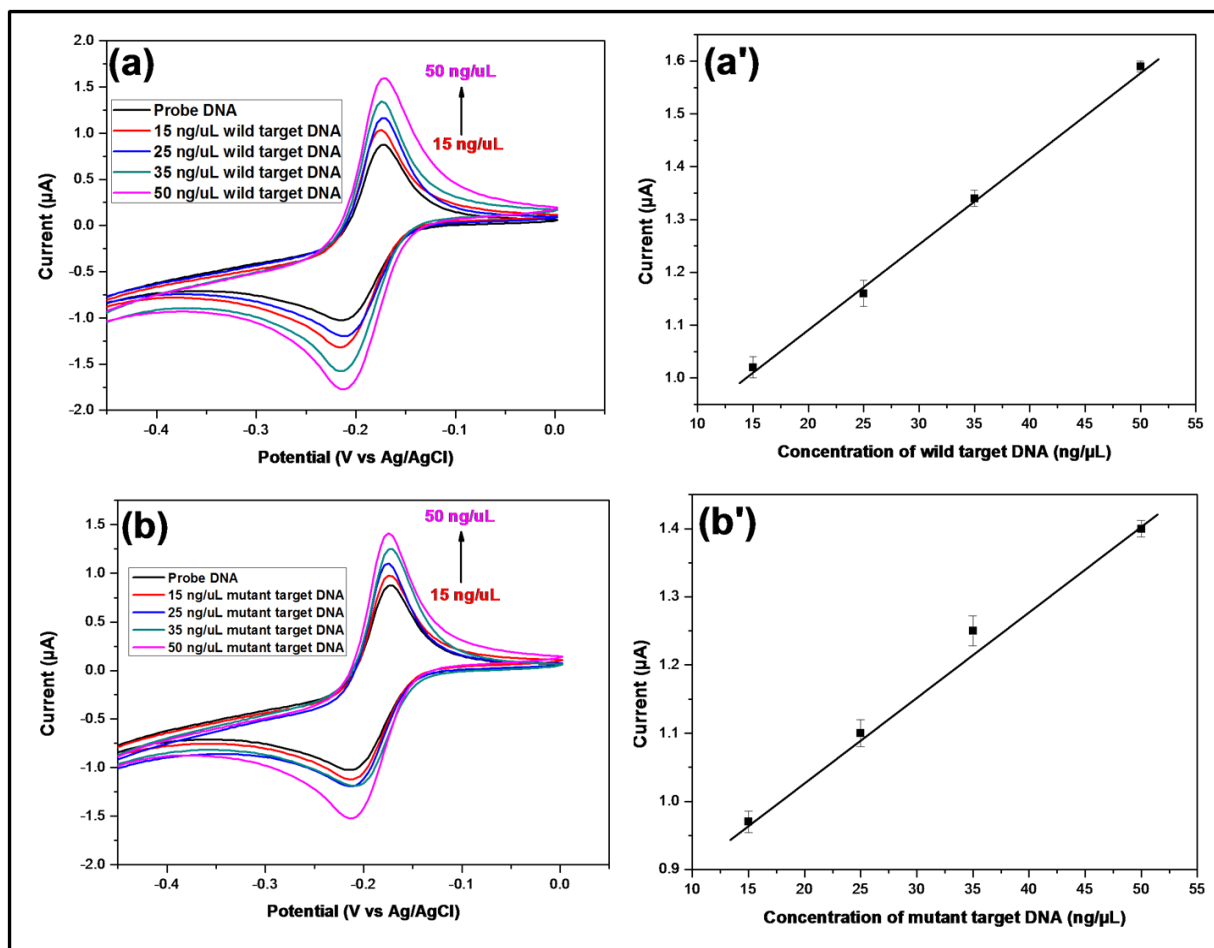


Figure 5. Cyclic voltammograms of ss-DNA-SH-Au electrode after hybridization with different concentrations of (a) wild and (b) mutant complementary DNA targets in PBS containing 40 μM methylene blue. Linear plots between current and concentrations of (a') wild and (b') mutant complementary DNA targets.

The Fig. 5a' and b' shows linear plots of current vs complementary target concentrations of wild and mutant type DNA, respectively. From this plot, the sensitivities of wild-ds-DNA-SH/Au and mutant-ds-DNA-SH/Au electrodes have been obtained as $0.0164 \mu\text{A}/\text{ng } \mu\text{L}^{-1}$ with 0.998 regression coefficient (R) and $0.0122 \mu\text{A}/\text{ng } \mu\text{L}^{-1}$ with 0.993 (R), respectively. The ssDNA-SH/Au electrode can detect wild and mutant type complementary target related to *FABP4* gene in the range of 5-10 $\text{ng } \mu\text{L}^{-1}$. Efforts are underway to use this ssDNA-SH/Au electrode for detecting SNP in PCR and genomic DNA of the *FABP4* gene.

4. CONCLUSIONS

The electrochemical SNP detection in *FABP4* gene biosensor has been fabricated by immobilization of ss-DNA-SH onto gold surfaces (ss-DNA-SH/Au). This ss-DNA-SH/Au electrode hybridized with wild and mutant complementary sequences related to *FABP4* gene in the presence methylene blue. The AFM, FT-IR, CV and impedance studies suggest that the ss-DNA-SH successfully immobilized onto the gold surfaces. The CV studies also reveal that the methylene blue accumulation is higher in the wild type target with respect to mutant type target. This result provides the present method has the capability to recognize the SNP in *FABP4* gene and also generating a type of an electrochemical biosensor for the sequence detection in DNA. The ss-DNA-SH/Au electrode is found to be stable for more than 3 months when stored at 4 °C. Efforts are underway to use this ssDNA-SH/Au electrode for detecting SNP in PCR and genomic DNA of the *FABP4* gene.

ACKNOWLEDGEMENTS

This research was supported by a WCU (World Class University) program through the National Research Foundation of Korea funded by the Ministry of Education, Science, and Technology (R32-20026).

References

1. R. M. Kaikaus, N. M Bass and R. K Ockner, *Experientia* 46 (1990) 617.
2. S. Hoashi, T. Hinenoya, A. Tanaka, H. Ohsaki, S. Sasazaki, M. Taniguchi, K. Oyama, F. Mukai and H. Mannen, *BMC genetics* 9 (2008) article No. 84.
3. S. H. Lee, J. H. J. van der Werf, S. H. Lee, E.W. Park, S. J. Oh, J.P. Gibson and J. M. Thomson, *Animal genetics* 41 (2010) 442.
4. P. Ross, L. Hall, I. Smirnov and L. Haff, *Nature biotechnology* 16 (1998) 1347.
5. D. Schmalzing, A. Belenky, M.A. Novotny, L. Koutny, O. Salas-Solano, S. El-Difrawy, A. Aram, P. Matsudaira and D. Ehrlich, *Nucleic acids research* 28 (2000) e43.
6. J. Li, X. Chu, Y. Liu, J. H. Jiang, Z. He, Z. Zhang, G. Shen and R. Q. Yu *Nucleic acids research* 33 (2005) e168.
7. Y. Li, A. W. Wark, H. J. Lee and R. M. Corn *Anal. Chem.* 78 (2006) 3158.
8. S. Cho, T. S. Park, D. H. Yoon, H. S. Cheong, S. Namgoong, B. L. Park, H. W. Lee, C. S. Han, E. M. Kim, I. C. Cheong, H. Kim and H. D. Shin, *BMB reports* 41 (2008) 29.
9. S. Zhang, Z. Wu, G. Shen and R. Yu, *Biosens. Bioelectron.* 24 (2009) 3201.
10. G.C. Zhao, J.J. Zhu and H. Y. Chen, *Spectrochimica acta, Part A: Molecular and biomolecular Spectroscopy* 55 (1999) 1109.
11. S. Nafisi, A.A. Saboury, N. Keramat, J. F. Neault and H. A. Tajmir-Riahi, *J. Mol. structure* 827 (2007) 35.
12. A. Erdem, K. Kerman, B. Meric, U. S. Akarca and M. Ozsoz, *Anal. Chim. acta* 422 (2000) 139.
13. W. R Yang, M. Ozsoz, D. B. Hibbert and J. J. Gooding, *Electroanalysis* 14 (2002) 1299.
14. H. Nasef, V. Beni, K. Ciara and O. Sullivan *Anal. Bioanal. Chem.* 396 (2010) 1423.
15. P. Oliver, K. Andreas and L. Fred *Biosens. Bioelectron.* 22 (2007) 2656.
16. O. K. Shana, M. J. Nicole, G. H. Michael, and K. B. Jacqueline, *Angewandte chemie* 38 (1999) 941.
17. M. K. Patel, P. R Solanki, S. Seth, S. Guptha, S. Khare, A. Kumar and B. D. Malhotra, *Electrochem. Commun.* 11 (2009) 969.

18. T. S. Ramulu, R. Venu, B. Sinha, S. S. Yoon and C. G. Kim, *Int. J. Electrochem. Sci.* 7 (2012) 7762.
19. T. S. Ramulu, R. Venu, B. Sinha, B. Lim S. J. Jeon S. S. Yoon and C. G. Kim, *Biosens. Bioelectron.* DOI:10.1016/j.bios.2012.07.034.
20. D. Maumita, S. Gajjala, R. Nagarajan and B. D. Malhotra *Appl. Phys. Lett.* 96 (2010) 133703.